

Core engagement with β -arrestin is dispensable for agonist-induced vasopressin receptor endocytosis and ERK activation

Punita Kumari^{a,†}, Ashish Srivastava^{a,†}, Eshan Ghosh^a, Ravi Ranjan^a, Shalini Dogra^b, Prem N. Yadav^b, and Arun K. Shukla^{a,*}

^aDepartment of Biological Sciences and Bioengineering, Indian Institute of Technology, Kanpur 208016, India;

^bDivision of Pharmacology, CSIR-Central Drug Research Institute, Lucknow, UP 226031, India

ABSTRACT G protein-coupled receptors (GPCRs) exhibit highly conserved activation and signaling mechanisms by which agonist stimulation leads to coupling of heterotrimeric G proteins and generation of second messenger response. This is followed by receptor phosphorylation, primarily in the carboxyl terminus but also in the cytoplasmic loops, and subsequent binding of arrestins. GPCRs typically recruit arrestins through two different sets of interactions, one involving phosphorylated receptor tail and the other mediated by the receptor core. The engagement of both set of interactions (tail and core) is generally believed to be necessary for arrestin-dependent functional outcomes such as receptor desensitization, endocytosis, and G protein-independent signaling. Here we demonstrate that a vasopressin receptor (V_2R) mutant with truncated third intracellular loop ($V_2R^{\Delta ICL3}$) can interact with β -arrestin 1 (β arr1) only through the phosphorylated tail without engaging the core interaction. Of interest, such a partially engaged $V_2R^{\Delta ICL3}$ - β arr1 complex can efficiently interact with clathrin terminal domain and ERK2 MAPK in vitro. Furthermore, this core interaction-deficient V_2R mutant exhibits efficient endocytosis and ERK activation upon agonist stimulation. Our data suggest that core interaction with β arr is dispensable for V_2R endocytosis and ERK activation and therefore provide novel insights into refining the current understanding of functional requirements in biphasic GPCR- β arr interaction.

Monitoring Editor

John York
Vanderbilt University

Received: Dec 8, 2016

Revised: Feb 13, 2017

Accepted: Feb 14, 2017

INTRODUCTION

G protein-coupled receptors (GPCRs), also known as seven-transmembrane receptors (7TMRs), constitute a large family of cell

This article was published online ahead of print in MBoC in Press (<http://www.molbiolcell.org/cgi/doi/10.1091/mbc.E16-12-0818>) on February 22, 2017.

[†]These authors contributed equally.

P.K. performed ELISA experiments, ERK assays, and coIP experiments (V_2R - β arr1-ERK2); A.S. performed bimane assays and coIP experiments (V_2R - β arr1; V_2R - β arr1-clathrin); E.G. and R.R. generated the receptor constructs and helped in various other aspects of the study; S.D. and P.N.Y. performed the GloSensor assay; A.K.S. supervised the overall project. All authors contributed to writing and editing the manuscript.

*Address correspondence to: Arun K. Shukla (arshukla@iitk.ac.in).

Abbreviations used: β arr, β -arrestin; EC_{50} , concentration of a drug that gives half-maximal response; ELISA, enzyme-linked immunosorbent assay; ERK, extracellular signal-regulated kinase; Fab, antigen-binding fragment; GPCR, G protein-coupled receptor; ICL3, third intracellular loop; MAPK, mitogen-activated protein kinase.

© 2017 Kumari, Srivastava, et al. This article is distributed by The American Society for Cell Biology under license from the author(s). Two months after publication it is available to the public under an Attribution-NonCommercial-Share Alike 3.0 Unported Creative Commons License (<http://creativecommons.org/licenses/by-nc-sa/3.0>).

"ASCB®," "The American Society for Cell Biology®," and "Molecular Biology of the Cell®" are registered trademarks of The American Society for Cell Biology.

surface proteins, with >800 members (Bjarnadottir et al., 2006). GPCRs display overall conserved 7TM architecture, activation mechanisms, signaling outcomes, and regulatory paradigms (Bockaert and Pin, 1999). Agonist binding results in conformational changes in the receptor, G protein coupling, and generation of second messengers such as Ca^{2+} , cAMP, and inositol triphosphate (Bockaert and Pin, 1999). This is followed by the phosphorylation of serine and threonine residues in the carboxyl terminus and intracellular loops by various kinases (Butcher et al., 2012; Gurevich et al., 2012). Activated and phosphorylated receptors recruit multifunctional adaptor proteins—arrestins—which are responsible for preventing further G protein coupling to the receptors and thereby desensitize the G protein response (Luttrell and Lefkowitz, 2002). There are four members in the arrestin family, arrestins-1–4; of these, arrestins-2 and 3 are also referred to as β -arrestin 1 (β arr1) and β -arrestin 2 (β arr2), respectively (Lefkowitz, 2007). In addition to terminating G protein signaling, β arrs are well established to mediate receptor endocytosis via a clathrin-dependent mechanism (Kang et al., 2014) and also trigger G protein-independent signaling responses downstream of

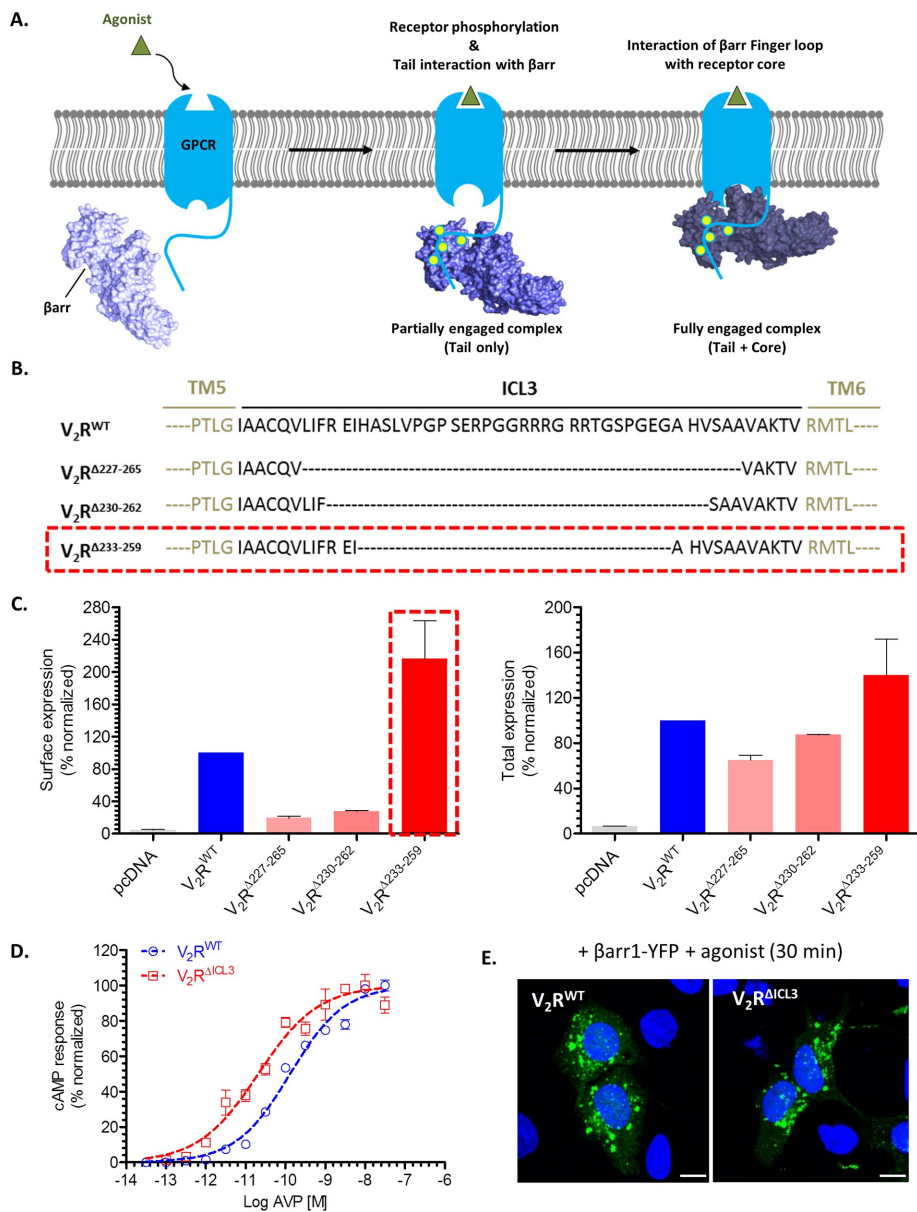


FIGURE 1: Characterization of a V_2R mutant with truncated ICL3 loop. (A) Schematic representation of biphasic GPCR- β arr interaction, which involves phosphorylated carboxyl terminus (receptor tail) and intracellular surface of the transmembrane receptor core. Here tail-only engaged receptor- β arr complex is referred to as “partially engaged complex,” and “fully engaged complex” refers to involvement of both set of interactions (tail plus core). (B) Schematic representation of three V_2R constructs containing truncated ICL3: $V_2R^{\Delta 227-265}$, $V_2R^{\Delta 230-262}$, and $V_2R^{\Delta 233-259}$. Black dotted lines indicate sequence that has been deleted. $V_2R^{\Delta 233-259}$ construct, highlighted by the red dashed box, is referred to as $V_2R^{\Delta ICL3}$. (C) N-terminal FLAG-tagged V_2R constructs were expressed in HEK-293 cells, and their surface and total expression was measured by a whole-cell ELISA as described in *Materials and Methods*. $V_2R^{\Delta 233-259}$ (referred to as $V_2R^{\Delta ICL3}$) exhibited robust surface expression, and therefore it was used in subsequent experiments. Expression data of V_2R constructs is normalized with respect to V_2R^{WT} , which is treated as 100%. pcDNA3.1 (empty vector)-transfected cells were used as a negative control. (D) Agonist-induced cAMP response downstream of V_2R^{WT} and $V_2R^{\Delta ICL3}$ in HEK-293T cells as measured by the GloSensor assay. Both V_2R^{WT} and $V_2R^{\Delta ICL3}$ exhibit robust cAMP generation, and the EC_{50} of $V_2R^{\Delta ICL3}$ is approximately an order of magnitude higher than that of V_2R^{WT} . Data represent two independent experiments each carried out in triplicate and normalized with respect to maximal response of V_2R^{WT} . (E) Confocal microscopy of HEK-293 cells expressing either V_2R^{WT} or $V_2R^{\Delta ICL3}$ with β arr1-YFP. Agonist stimulation leads to accumulation of endocytotic vesicles, which indicates recruitment of β arr1 to activated receptor and subsequent receptor internalization. Scale bar, 10 μ m.

activated GPCRs (DeWire *et al.*, 2007; Shenoy and Lefkowitz, 2011; Srivastava *et al.*, 2015). β arrs mediate receptor desensitization by sterically hindering G protein coupling to the receptor (Farrens *et al.*, 1996; Rasmussen *et al.*, 2011; Szczepek *et al.*, 2014; Kang *et al.*, 2015), and their ability to facilitate receptor endocytosis and G protein-independent signaling arises primarily from their scaffolding properties (Lefkowitz and Shenoy, 2005; DeWire *et al.*, 2007). For example, β arrs can scaffold components of endocytosis machinery such as clathrin and β 2 adaptin subunit of AP2 to mediate agonist-induced GPCR endocytosis (Goodman *et al.*, 1996; Laporte *et al.*, 1999). However, for some GPCRs, β arr-independent endocytosis has also been reported (van Koppen and Jakobs, 2004). Similarly, β arrs can also scaffold various components of extracellular signal-regulated kinase (ERK) mitogen-activated protein kinase (MAPK) cascades, such as Raf1, MEK1, and ERK2, in order to facilitate G protein-independent ERK MAPK activation (Luttrell *et al.*, 2001; Coffa *et al.*, 2011).

Arrestins interact with GPCRs through two sets of interactions, one involving the phosphorylated carboxyl terminus of the receptor (also referred to as the receptor tail) and the other involving the receptor core (Gurevich and Gurevich, 2004, 2013; Shukla *et al.*, 2014). A recently determined crystal structure of β arr1 bound to a phosphopeptide corresponding to the carboxyl terminus of the vasopressin receptor (V_2R) has directly revealed the interaction of receptor-attached phosphates with positively charged residues in the N-domain of β arr1 (Shukla *et al.*, 2013). In addition, the crystal structure of a rhodopsin-arrestin-1 fusion protein identified the regions in the receptor and arrestin-1 involved in making the core interaction (Kang *et al.*, 2015, 2016). Furthermore, a combination of single-particle electron microscopy (EM), hydrogen-deuterium exchange, and cross-linking resulted in direct visualization of biphasic interaction between a modified β 2-adrenergic receptor (β 2AR) and β arr1 (Shukla *et al.*, 2014; Figure 1A). It is generally believed that complete engagement of β arrs with GPCRs involving both the tail and the core interaction is likely to be required for functional outcomes. However, previous studies reported that interaction with isolated phosphopeptides corresponding to the carboxyl terminus of GPCRs is sufficient to trigger activation-dependent conformational changes in arrestins (Puig *et al.*, 1995; Xiao *et al.*, 2004; Nobles *et al.*, 2007). For β arrs, binding of phosphopeptide also

results in enhanced interaction with clathrin heavy chain in vitro (Xiao *et al.*, 2004; Nobles *et al.*, 2007). In addition, crystallization attempts of p44, a carboxyl-terminus-truncated splice variant of arrestin-1, with phosphorylated opsin also resulted in an “active-like” conformation in the crystal structure despite the lack of cocrystallization with opsin (Kim *et al.*, 2013). This observation suggests that transient interaction with phosphorylated receptor might be sufficient to prime arrestin-1 activation. Finally, single-particle EM analysis of a complex of β arr1 with a modified β_2 AR stabilized with an antibody fragment revealed a significant population in which the receptor and β arr1 are associated only through the phosphorylated receptor tail (Shukla *et al.*, 2014). This observation suggests that physical formation of a receptor- β arr complex may not necessarily require the core interaction. Taken together, these data indicate that engagement of arrestins to phosphorylated receptor tail even in the absence of the core interaction might be sufficient to trigger some functional outcomes.

We recently demonstrated that for a chimeric β_2 -adrenergic receptor that harbors the carboxyl terminus of the vasopressin receptor (referred to as β_2 V₂R), engagement of the core interaction with β arr1 is not required for endocytosis and ERK MAPK activation (Kumari *et al.*, 2016). However, it remains unclear whether even for a native GPCR, full engagement with β arrs may not be essential for functional outcomes. Accordingly, here we sought to isolate a partially engaged complex of β arr1 with the human V₂R associated only through the phosphorylated carboxyl terminus and compare its functional properties with a fully engaged V₂R- β arr1 complex in vitro and in a cellular context. We found that a V₂R construct defective in making the core interaction not only forms a stable complex with β arr1 in solution but also efficiently undergoes agonist-induced endocytosis and triggers ERK MAPK activation.

RESULTS AND DISCUSSION

A V₂R mutant with truncated third intracellular loop efficiently recruits β arr1

Chemical cross-linking on a preformed β_2 V₂R- β arr1 complex using a heterobifunctional amine-reactive cross-linker and a disulfide trapping strategy identified close proximity between the third intracellular loop (ICL3) in the receptor and the finger loop in β arr1 (Shukla *et al.*, 2014). Similarly, the crystal structure of rhodopsin-arrestin-1 fusion protein and site-specific disulfide cross-linking experiments also suggest that ICL3 in the receptor and finger loop in arrestin-1 are closely positioned during their interaction (Kang *et al.*, 2015). Because this proximal positioning of receptor ICL3 and β arr finger loop forms a key interface for the core interaction, we hypothesized that V₂R mutants with truncated ICL3 may not engage the core interaction with β arrs. Complexes of such V₂R mutants with β arr1, if formed, should represent partially engaged complexes involving only the tail interaction (i.e., through the phosphorylated carboxyl terminus). Accordingly, we first generated a series of ICL3-truncated V₂R constructs (Figure 1B) and measured their total and surface expression in transfected HEK-293 cells using a cell-based enzyme-linked immunosorbent assay (ELISA; Figure 1C). We observed that a V₂R construct with H²³³-G²⁵⁹ truncation in ICL3 expresses robustly at the cell surface (Figure 1, B and C, red dotted box). We refer to this construct as V₂R^{ΔICL3} and used it in subsequent experiments. Agonist stimulation of HEK-293T cells expressing V₂R^{ΔICL3} resulted in robust generation of cAMP, and, of interest, the EC₅₀ of cAMP generation for V₂R^{ΔICL3} was ~5- to 10-fold higher than that for wild type (WT), V₂R^{WT} (Figure 1D). This observation indicates relatively more efficient coupling of G α s to V₂R^{ΔICL3} than with V₂R^{WT}.

Next we tested whether V₂R^{ΔICL3}, potentially deficient in engaging the core interaction with β arrs, exhibits detectable physical interaction with β arr1. Confocal microscopy of HEK-293 cells expressing β arr1-yellow fluorescent protein (YFP) revealed robust interaction of V₂R^{ΔICL3} with β arr1, as apparent by the formation of endocytotic vesicles upon agonist stimulation, similar to V₂R^{WT} (Figure 1E). This observation suggests that truncation of ICL3 and, presumably, therefore the loss of core interaction do not adversely affect the formation of a stable receptor- β arr1 complex in the cellular context. To further corroborate this finding and establish the lack of core engagement in the V₂R^{ΔICL3}- β arr1 complex, we expressed and purified V₂R^{WT} and V₂R^{ΔICL3} using cultured Sf9 cells. To trigger receptor phosphorylation and generate purified receptor protein harboring phosphorylated carboxyl terminus, we also coexpressed a membrane-tethered GRK2^{CAAX} construct in these cells. Before harvesting the cells for receptor purification, we stimulated them with agonist (AVP) to trigger V₂R phosphorylation. Assembling a V₂R- β arr1 complex in vitro was technically not feasible due to the transient nature of this complex, and therefore, to stabilize this complex, we used a previously described synthetic antibody fragment referred to as antigen-binding fragment 30 (Fab30). This Fab selectively recognizes an active conformation of β arr1 induced by the binding of V₂Rpp (a phosphopeptide corresponding to the carboxyl terminus of V₂R), and we successfully used it previously to assemble a stable complex of β arr1 with β_2 V₂R in vitro (Shukla *et al.*, 2014; Kumari *et al.*, 2016). Using the ELISA-based approach depicted in Figure 2A, we successfully reconstituted a stable complex of V₂R^{WT} and β arr1 (Figure 2, B–D). This complex is sensitive to receptor phosphorylation state, as agonist-bound but dephosphorylated receptor does not display stable complex formation even in the presence of Fab30 (Figure 2B). In line with confocal microscopy data, V₂R^{ΔICL3} also exhibited robust complex formation with β arr1, as assessed by ELISA (Figure 2, C and D) and coimmunoprecipitation assay (coIP; Figure 2, E and F). These observations taken together establish that a stable V₂R^{ΔICL3}- β arr1 complex can be reconstituted in vitro.

Bimane fluorescence spectroscopy reveals lack of core interaction in the V₂R^{ΔICL3}- β arr1 complex

To test the status of the core engagement in the V₂R^{ΔICL3}- β arr1 complex, we used bimane fluorescence spectroscopy. As mentioned earlier, the finger loop of β arr1 is a key component of the core interaction with the receptor (Figure 3A). Therefore we used a previously described single-cysteine mutant of β arr1 harboring a cysteine at position 68 in the finger loop, referred to as β arr1^{L68C} (Kumari *et al.*, 2016), and chemically labeled it with an environmentally sensitive fluorophore, monobromobimane (mBBr). We reasoned that the core interaction, which involves docking of the finger loop to the intracellular surface of the receptor, should lead to a change in fluorescence intensity and therefore can be used as a readout of the core interaction (Figure 3A). In fact, finger loop-labeled visual arrestin has been used extensively to study its interaction with activated and phosphorylated rhodopsin (Sommer *et al.*, 2005, 2007; Sinha *et al.*, 2014), and we have also used bimane labeled β arr1^{L68C} to investigate the core interaction between the β_2 V₂R and β arr1 (Kumari *et al.*, 2016). In line with our hypothesis, interaction of V₂R^{WT} with bimane-labeled β arr1 led to a significant quenching of the fluorescence intensity, indicating core engagement (Figure 3, B and C). In contrast, interaction of V₂R^{ΔICL3} did not yield any detectable decrease in bimane fluorescence, although it forms a physically stable complex with β arr1, as presented in Figure 2, C–F. As a control, incubation of inactive and

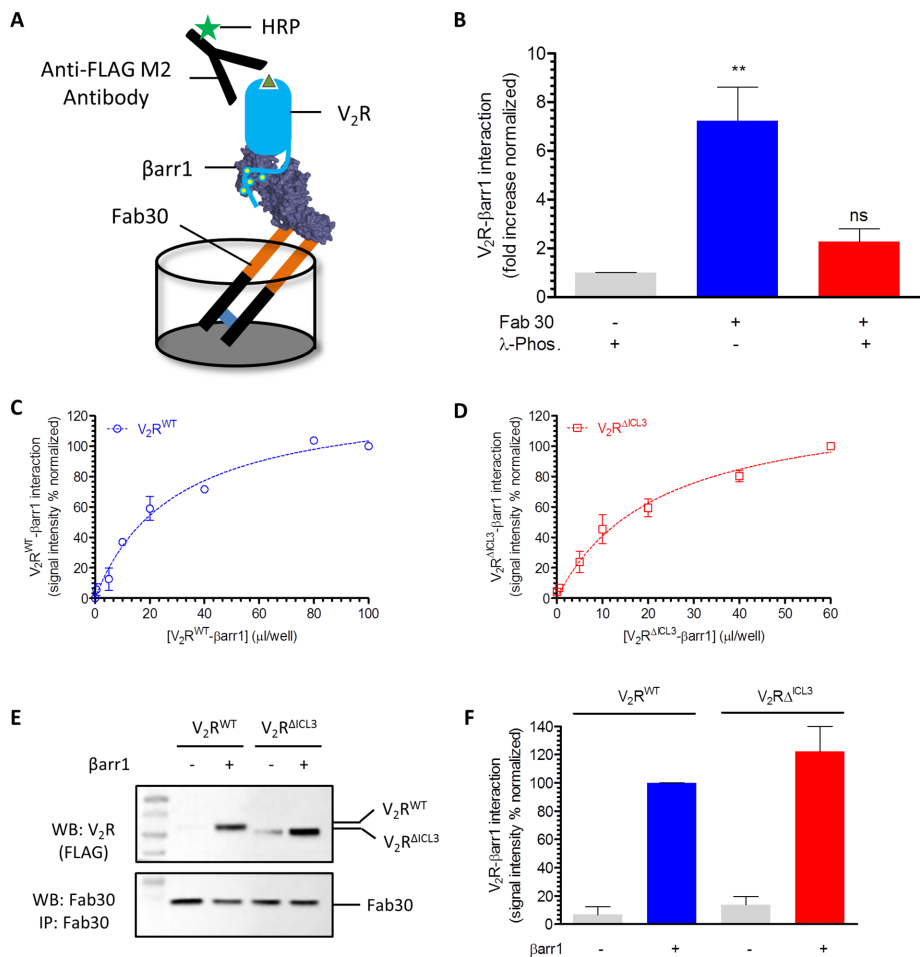


FIGURE 2: $V_2R^{\Delta ICL3}$ interacts efficiently with β arr1 in vitro. (A) Schematic representation of an ELISA format for assembling V_2R - β arr1 complex in vitro. Purified Fab30, an antibody fragment that selectively recognizes activated β arr1 conformation, is used as an anchor to stabilize the complex. Formation of the complex is visualized using M2 antibody against the FLAG tag at the N-terminus of the receptor. (B) Stable formation of V_2R - β arr1 complex requires Fab 30 and is sensitive to receptor phosphorylation. Dephosphorylated receptor (with λ -phosphatase [λ -Phos]) does not exhibit detectable complex formation. Data from four independent experiments are normalized with respect to the basal signal observed without Fab30 immobilization (treated as 1) and analyzed using one-way analysis of variance (ANOVA) with Bonferroni posttest (** $p < 0.01$). (C) Fab30-stabilized in vitro assembly of V_2R^{WT} - β arr1 complex as assessed by ELISA using cell lysate from Sf9 cells expressing V_2R^{WT} following the protocol described in *Materials and Methods*. Here a fixed amount of Fab30 was first immobilized in the ELISA plate, followed by the addition of various amounts of V_2R^{WT} - β arr1 mixture and subsequent detection of complex formation by HRP-coupled M2 antibody. (D) Similar to V_2R^{WT} , $V_2R^{\Delta ICL3}$ also exhibits robust interaction with β arr1 upon stabilization using Fab30 as assessed by ELISA. Data in C and D represent two independent experiments each carried out in duplicate and normalized with respect to the maximal response (treated as 100%). (E) Fab30-stabilized formation of β arr1 complexes for V_2R^{WT} and $V_2R^{\Delta ICL3}$ as assessed by colP using purified proteins. The image is a representative blot of four independent experiments. (F) Densitometry-based quantification of V_2R - β arr1-Fab30 complex formation using colP data in E. Data are normalized with respect to the signal obtained for V_2R^{WT} plus β arr1 condition (treated as 100%).

nonphosphorylated V_2R , which does not interact with β arr1, did not change the bimane fluorescence in this assay. Taken together, these data establish that the $V_2R^{\Delta ICL3}$ - β arr1 complex is associated only through the carboxyl terminus and does not engage the core interaction. Therefore V_2R^{WT} - β arr1 and $V_2R^{\Delta ICL3}$ - β arr1 complexes represent fully engaged (i.e., core plus tail) and partially engaged (i.e., tail alone) complexes, respectively.

Partially engaged $V_2R^{\Delta ICL3}$ - β arr1 complex binds clathrin and supports receptor internalization

As mentioned earlier, one of the key functions of β arrs is to mediate clathrin-dependent endocytosis of GPCRs upon agonist stimulation (Kang et al., 2014). β arrs bind to clathrin heavy chain and facilitate the trafficking of activated receptors in clathrin-coated vesicles (Goodman et al., 1996). Therefore, to test the functional competence of partially engaged $V_2R^{\Delta ICL3}$ - β arr1 complex (i.e., associated only through the receptor tail), we first measured its interaction with the clathrin heavy-chain terminal domain (TD). We used a single-chain version of Fab30, referred to as ScFv30, to stabilize V_2R^{WT} - β arr1 and $V_2R^{\Delta ICL3}$ - β arr1 complexes to avoid potential steric clash with clathrin binding. As presented in Figure 4, A and B, colP revealed that even the partially engaged complex ($V_2R^{\Delta ICL3}$ - β arr1) binds effectively to clathrin TD, similar to the fully engaged complex (V_2R^{WT} - β arr1). Of greater importance, assessment of agonist-triggered receptor internalization in HEK-293 cells also revealed comparable endocytosis of V_2R^{WT} and $V_2R^{\Delta ICL3}$ (Figure 4C). These findings suggest that the core interaction in V_2R - β arr1 complex is dispensable for clathrin binding and β arr-mediated receptor internalization.

Partially engaged $V_2R^{\Delta ICL3}$ - β arr1 complex binds ERK MAPK and supports ERK activation

In addition to classical G protein-dependent signaling, parallel signaling pathways mediated by β arrs have also been identified for a number of GPCRs, and it has now become a generally applicable paradigm in the GPCR family (Lefkowitz and Shenoy, 2005; DeWire et al., 2007). β arrs can nucleate various signaling assemblies to facilitate their activation and trigger specific signaling pathways (Luttrell et al., 1999; McDonald et al., 2000; Lin and DeFea, 2013). For example, β arrs can scaffold various components of ERK MAPK cascade, such as Raf1, MEK1, and ERK2, which leads to ERK phosphorylation and activation (DeWire et al., 2007; Coffa et al., 2011; Gurevich and Gurevich, 2013, 2014). Therefore we first investigated the ability of the partially engaged complex to

interact with inactive (nonphosphorylated) and active (phosphorylated) ERK2. Similar to clathrin binding, we observed that the partially engaged complex ($V_2R^{\Delta ICL3}$ - β arr1; stabilized by ScFv30) robustly interacted with inactive and active ERK2, similar to fully engaged complex (Figure 5, A and B). Agonist-induced ERK activation downstream of GPCRs exhibits a biphasic pattern in which the early phase depends primarily on G protein activation, whereas the

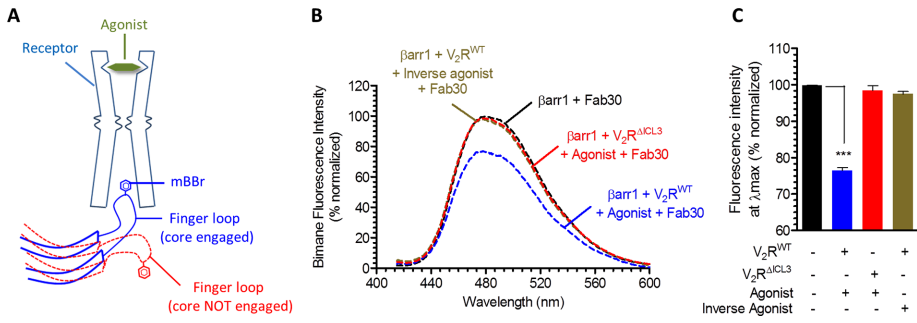


FIGURE 3: Fluorescence spectroscopy reveals that $V_2R^{\Delta ICL3}$ - β arr1 complex lacks the core interaction. (A) Schematic representation of bimane fluorescence quenching assay as a readout of the core interaction between V_2R and β arr1. The finger loop of β arr1 is labeled with mBBr, and the core interaction with receptor leads to a decrease in bimane fluorescence intensity. (B) Bimane fluorescence of β arr1 decreases upon its interaction with V_2R^{WT} suggesting the engagement of the core interaction. Of interest, however, for $V_2R^{\Delta ICL3}$, there is no decrease in bimane fluorescence, suggesting the lack of core interaction, which confirms that the $V_2R^{\Delta ICL3}$ - β arr1 complex is partially engaged, that is, associated only through the receptor tail. Here V_2R - β arr1 complexes are stabilized with Fab30, and AVP and tolaptan were used as agonist and inverse agonist, respectively. Purified receptors are preincubated with excess molar concentration of indicated ligands, followed by incubation with β arr1^{mBBr} and Fab30. (C) Bimane fluorescence intensity at λ_{max} as measured in B. Data were analyzed using one-way ANOVA with Bonferroni posttest ($***p < 0.001$). Data in B and C represent an average of three independent experiments.

late phase is mediated primarily by β arrs (DeWire *et al.*, 2007). This temporal pattern of ERK activation has been directly visualized for V_2R as well, using H-89 (PKA inhibitor) and small interfering RNA-mediated knockdown of β arrs (Ren *et al.*, 2005). ERK activation after 5 min of agonist stimulation was sensitive to H-89, indicating predominant dependence on $G_{\alpha s}$ (and cAMP), whereas that at 10 min and beyond was sensitive to β arr knockdown (Ren *et al.*, 2005). Therefore we measured agonist-induced ERK activation in HEK-293 cells expressing $V_2R^{\Delta ICL3}$ or V_2R^{WT} and observed that they displayed comparable levels of ERK activation at 5, 15, and 30 min after agonist stimulation (Figure 5, C and D). These findings suggest that, similar to clathrin binding and receptor endocytosis, interaction of

ERK2 and β arr-dependent ERK activation also do not require core engagement between β arr and V_2R . Interaction of β arrs with activated and phosphorylated receptors is a hallmark of GPCR family members. Although primary sequence of GPCRs is not highly conserved, most of them, if not all, undergo agonist-induced phosphorylation and display conserved conformational rearrangement during activation (Manglik and Kobilka, 2014). These two features are most likely responsible for β arrs interacting with and regulating a large repertoire of GPCRs. It is also interesting that functional aspects of the GPCR- β arr interaction, such as receptor desensitization, endocytosis, and G protein-independent signaling, are also mostly conserved. Comparison of rhodopsin-arrestin-1 fusion protein crystal structure (Kang *et al.*, 2015) and β_2AR -Gs crystal structure (Rasmussen *et al.*, 2011) reveals significant overlapping interface for arrestin and G αs binding on the receptor and corroborates a steric hindrance-based receptor desensitization mechanism. In this context, it is interesting that EC_{50} of agonist-induced cAMP generation for $V_2R^{\Delta ICL3}$ is about an order of magnitude higher than that of V_2R^{WT} (Figure 1D). This suggests more efficient G protein coupling and/or less efficient desensitization of $V_2R^{\Delta ICL3}$ than with V_2R^{WT} and therefore directly indicates that the core interaction with β arr is critical for mediating receptor desensitization.

The crystal structure of β arr1 in complex with V_2R_{pp} directly reveals major conformational changes in β arr1 consistent with the notion that interaction of receptor attached phosphates can drive an "active-like" β arr conformation (Shukla *et al.*, 2013). Furthermore, direct visualization of a stable, tail only-engaged β_2V_2R - β arr1 complex (Shukla *et al.*, 2014) and previous studies demonstrating enhanced clathrin binding to V_2R_{pp} -occupied β arrs (Xiao *et al.*, 2004; Nobles *et al.*, 2007) raise the possibility that even partially engaged intermediates during biphasic GPCR- β arr interaction might be able to drive some of the β arr functions. Here we discover that a complex of β arr1 with a V_2R mutant lacking the core interaction can efficiently bind clathrin and ERK MAPK. Moreover, this V_2R mutant also efficiently undergoes agonist-dependent internalization and triggers ERK MAPK activation identical to the WT receptor in cells. As mentioned earlier, most signaling and regulatory paradigms in GPCR family are generally conserved. Therefore it is tempting to speculate that the dispensability of the core interaction for at least some of the functional outcomes might also be applicable to other receptors. Considering the broad functional repertoire of β arrs, it would also be very interesting to investigate whether majority of β arr functions other than desensitization can be mediated by partially engaged complexes.

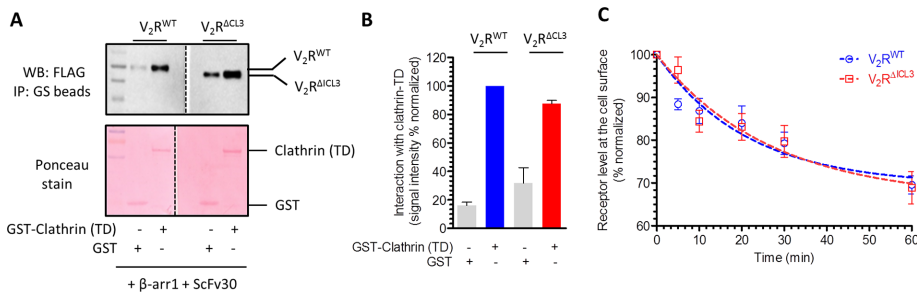


FIGURE 4: $V_2R^{\Delta ICL3}$ - β arr1 complex binds clathrin, and $V_2R^{\Delta ICL3}$ undergoes efficient endocytosis. (A) A coIP experiment reveals that $V_2R^{\Delta ICL3}$ - β arr1 complex (partially engaged) is able to interact with GST-clathrin-TD, similar to V_2R^{WT} - β arr1 complex (fully engaged). Here ScFv30 is used to stabilize V_2R - β arr1 complexes to avoid any potential clash with clathrin binding. Purified GST is used as a negative control. A representative image of four independent experiments. (B) Densitometry-based quantification of coIP data in A. Data are normalized with respect to clathrin interaction with V_2R^{WT} - β arr1 complex (treated as 100%). (C) Agonist-induced endocytosis of V_2R^{WT} and $V_2R^{\Delta ICL3}$ are comparable, suggesting that the inability of $V_2R^{\Delta ICL3}$ to engage the core interaction with β arr does not affect receptor endocytosis. Here HEK-293 cells expressing either V_2R^{WT} or $V_2R^{\Delta ICL3}$ were stimulated with 100 nM AVP (agonist) for indicated times, and the loss of surface receptor as measured by reactivity of HRP-coupled M2 antibody with N-terminal FLAG tag in whole-cell ELISA was used as a readout of receptor endocytosis. Data represent average \pm SEM of six independent experiments each carried out in duplicate.

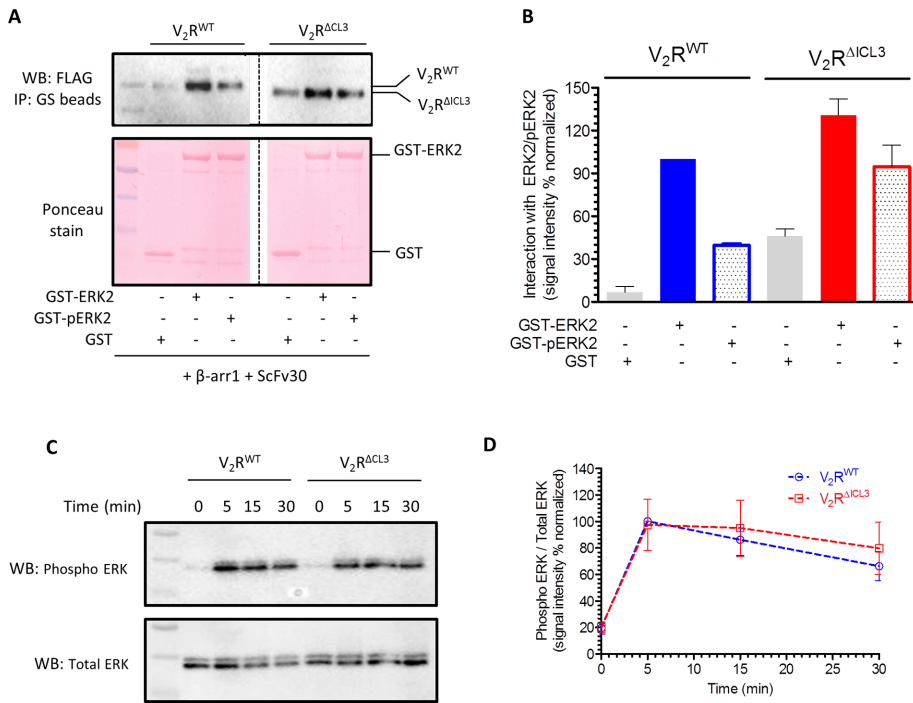


FIGURE 5: V₂R^{ΔICL3}-βarr1 complex binds ERK2, and V₂R^{ΔICL3} exhibits efficient ERK activation. (A) V₂R^{ΔICL3}-βarr1 complex interacts efficiently with inactive (i.e., nonphosphorylated) and active (i.e., phosphorylated) ERK2, similar to V₂R^{WT}-βarr1 complex, as assessed by a coIP experiment. Here ScFv30 is used to stabilize V₂R-βarr1 complexes to avoid any potential clash with ERK2 binding. Purified GST is used as negative control. Representative image of three independent experiments. (B) Densitometry-based quantification of coIP data presented in A, showing the interaction of inactive and active ERK2 with preformed V₂R^{WT/ΔICL3}-βarr1 complexes. Data are normalized with respect to the signal observed for the interaction of inactive ERK2 with V₂R^{WT}-βarr1 complex (treated as 100%). (C) Agonist (100 nM AVP)-stimulated ERK activation in HEK-293 cells expressing V₂R^{WT} or V₂R^{ΔICL3} as measured by Western blotting. V₂R^{ΔICL3} exhibits efficient ERK activation similar to V₂R^{WT}, indicating that the lack of core interaction with βarr does not influence ERK phosphorylation. A representative image from six independent experiments. (D) Densitometry-based quantification of agonist-induced ERK phosphorylation in C. Data represent average ± SEM of six independent experiments normalized with respect to signal at 5 min for V₂R^{WT} (treated as 100%).

In conclusion, our data establish that even a partially engaged V₂R-βarr complex lacking the core interaction is functional with respect to receptor endocytosis and ERK activation. Our findings also support the requirement of core interaction for steric hindrance-based receptor desensitization. Taken together, our observations reveal a functional segregation associated with the tail and the core interaction between GPCRs and βarrs and provide novel insights into biphasic GPCR-βarr interaction. As mentioned earlier, a key aspect of the broad functional repertoire of βarrs is their ability to scaffold a large number of interaction partners, and therefore it would be interesting to explore which of these interactions and corresponding functions, if any, might still require a core interaction between GPCRs and βarrs.

MATERIALS AND METHODS

General chemicals, plasmids, cell culture, and recombinant protein expression

General reagents used in this study were purchased from Sigma-Aldrich unless specified otherwise. Antibodies used in this study were anti-FLAG M2-horseradish peroxidase (HRP) conjugated (A8592; Sigma-Aldrich), anti-pERK2 (1:5000; 9101 Cell Signaling Technology), and anti-tERK2 (1:5000; 9102; Cell Signaling Technology). The

coding region of the human V₂R was synthesized (GenScript) and cloned into pcDNA3.1 with an N-terminal FLAG tag, and V₂R^{ΔICL3} construct was generated using overlap extension PCR. Plasmid constructs for bacterial expression of Fab30, ScFv30, βarr1, βarr1^{L68C}, clathrin (TD), and ERK2 were described previously (Kumari et al., 2016). The βarr1-YFP plasmid construct for expression in HEK-293 cells was also described earlier (Kumari et al., 2016). All constructs were sequence validated (Macrogen).

HEK-293 cells were grown in DMEM (Sigma-Aldrich), maintained under 5% CO₂, and transfected with polyethylenimine (PEI) using standard protocols. For purification of phosphorylated V₂R^{WT} and V₂R^{ΔICL3}, receptor-coding regions were first subcloned into pVL1393 with N-terminal FLAG tag, and baculovirus stocks were generated using standard protocols (Expression Systems). Cultured Sf9 cells were infected with virus stocks corresponding to either the V₂R^{WT} or V₂R^{ΔICL3} together with GRK2^{CAAX} at a density of 1.5 × 10⁶ cells/ml. At 60–66 h postinfection, cells were stimulated with 100 nM AVP for 1 h at 37°C to induce receptor phosphorylation and subsequently harvested by centrifugation. Recombinant receptors were solubilized with maltose neopentyl glycol (MNG; 0.5% wt/vol) and purified using anti-FLAG M1 antibody affinity resin following a similar protocol as described previously for β₂V₂R (Kumari et al., 2016). Purified receptor preparations were flash frozen with 10% glycerol and stored at -80°C until further use.

Whole-cell ELISA for measuring surface expression of V₂R^{WT} and V₂R^{ΔICL3}

Surface and total expression of V₂R constructs were measured using a previously published whole-cell ELISA-based protocol (Kumari et al., 2016). This assay essentially measures the reactivity of an anti-FLAG M2 antibody to cells expressing N-terminal FLAG-tagged receptor constructs. Here the signal arising from nonpermeabilized cells indicates surface expression, and the signal arising from permeabilized cells represent total (surface plus internal) receptor levels. HEK-293 cells were transfected with either WT V₂R or various truncated V₂R constructs (as indicated in Figure 1C) using PEI. At 24 h posttransfection, cells were seeded into poly-D-lysine-coated 24-well plates. After another 24 h, cells were serum starved for 1 h, washed with ice-cold Tris-buffered saline (TBS), fixed with 4% (wt/vol) paraformaldehyde (PFA) on ice, and washed again with TBS. Afterward, cells were incubated with blocking buffer (TBS plus 1% bovine serum albumin [BSA]) for 90 min at room temperature. To measure total receptor expression, cells were permeabilized with 0.01% Triton X-100 during the blocking step. Subsequently cells were incubated with HRP-coupled anti-FLAG M2 antibody (1.5–2 h at room temperature) and then washed three times with TBS plus 1% BSA. Finally, receptor expression was visualized by adding 3,3',5,5'-tetramethylbenzidine (TMB) ELISA, and the reaction was stopped by adding 1 M H₂SO₄. Signal intensities were taken at 450 nm. For normalization of total cell numbers in

each well, cells were washed with TBS (after TMB ELISA signals were measured), incubated with 0.2% (wt/vol) Janus Green dye (mitochondrial stain) for 10 min, and then destained with water. The color was developed by adding 0.5 M HCl, and the absorbance was measured at 595 nm. The ratio of A_{450} (TMB ELISA) to A_{595} (Janus Green) was used to calculate surface and total expression of V_2R constructs (Figure 1C). Overall surface expression levels of V_2R^{WT} and $V_2R^{\Delta ICL3}$ were comparable.

GloSensor assay

To measure agonist-induced G protein coupling and cAMP generation for V_2R^{WT} and $V_2R^{\Delta ICL3}$ (Figure 1D), HEK-293T cells were cotransfected with plasmids for the receptor and the luciferase-based cAMP biosensor (total 0.1 $\mu\text{g}/\text{well}$ in 96-well plate; pGloSensorTM-22F plasmid; Promega) using PEI. Transfected cells were incubated for 14–16 h, followed by removal of the cell culture medium and addition of 100 μl of sodium luciferin solution to cells in ligand buffer (1 \times Hanks balanced salt solution, pH 7.4, and 20 mM 4-(2-hydroxyethyl)-1-piperazineethanesulfonic acid [HEPES]). Subsequently plates were incubated at 37°C for 90 min, and then indicated concentrations of AVP (100 nM to 0.1 pM serially diluted in half log) were added to cells. After an additional incubation for 10–15 min, luminescence readings in wells were recorded using a luminescence plate reader (BMG LabTech). Data were corrected with respect to vehicle control, and normalized with respect to maximal stimulation by agonist (treated as 100%). Data were plotted and analyzed using nonlinear regression in GraphPad Prism software.

Confocal microscopy

For visualization of agonist-stimulated recruitment of $\beta\text{arr1-YFP}$ (Figure 1E), transfected HEK-293 cells were seeded onto 0.001% poly-D-lysine-coated glass coverslips and serum starved for 4 h. Cells were then stimulated with 100 nM AVP for the indicated time point, fixed using 4% PFA, and permeabilized with 0.01% Triton X-100. For nuclear staining, 0.5 $\mu\text{g}/\text{ml}$ 4',6-diamidino-2-phenylindole solution (Sigma-Aldrich) was added to fixed cells. After a final wash with PBS, coverslips were mounted onto glass slides using VectaShield H-1000 mounting medium (VectaShield), allowed to air dry for 15 min, and then imaged using an LSM780NLO confocal microscope (Carl Zeiss).

Formation of V_2R^{WT} - βarr1 and $V_2R^{\Delta ICL3}$ - βarr1 complexes and their interaction with clathrin and ERK2

These complexes were assembled in ELISA and coIP format following a previously published experimental setup (Kumari et al., 2016). Briefly, for ELISA-based assembly (Figure 2, A–D), purified Fab30 was first immobilized in a MaxiSorp ELISA plate, followed by incubation of wells with 5% BSA to block nonspecific binding. Subsequently lysates from *Sf9* cells expressing recombinant receptor constructs and purified βarr1 were added to immobilized Fab30 in ELISA plates. *Sf9* cells were stimulated with agonist (AVP, 100 nM) before preparation of the lysate in order to induce receptor activation and phosphorylation. As a control, cell lysate was incubated with λ -phosphatase to remove receptor phosphorylation (Figure 2B). Subsequently the plate was incubated at room temperature (25°C) for 1 h, followed by extensive washing of the wells and incubation with HRP-coupled anti-FLAG M2 antibody (1:2000) for 1 h. After additional washing, signal was detected using TMB ELISA solution (GenScript), the reaction was stopped by adding 1 M H_2SO_4 , and the signal was recorded at 450 nm in a multimode Plate Reader (PerkinElmer). For the saturation-binding experiment in Figure 2, C and D, immobilized Fab30 was incubated with various concentra-

tions of the receptor (in the form of cell lysate) and βarr1 (purified protein). For these experiments, ~24 ml of *Sf9* cells (60–66 h postinfection) were lysed in 1.5 ml of lysis buffer (20 mM HEPES, pH 7.4, 100 mM NaCl, 0.5% MNG) and mixed with 80–100 μg of βarr1 , and indicated volumes of lysate plus βarr1 mixture were added to each well of the ELISA plate.

To assess the formation of V_2R - βarr1 complexes in solution by coIP (Figure 2E), purified V_2R (WT and ΔICL3) was mixed with purified βarr1 and Fab30 and incubated at room temperature for 1 h; subsequently 20 μl of protein L beads was added. Afterward, beads were washed three times (20 mM HEPES, pH 7.4, 100 mM NaCl, 0.01% MNG), eluted with SDS loading buffer, and used for Western blotting-based detection of V_2R - βarr1 interaction.

To measure the binding of clathrin and ERK2 with preformed complexes (Figures 4, A and B, and 5, A and B), purified glutathione S-transferase (GST)-clathrin-TD/GST-ERK2/GST-pERK2 were first captured on GS beads, followed by incubation with preformed V_2R - βarr1 -ScFv30 complexes. After three rounds of washing, bound proteins were eluted in SDS loading buffer and probed by Western blotting using HRP-coupled anti-FLAG M2 antibody. Purified GST was used as a control for nonspecific binding of the complex to GS beads. Densitometry-based quantification of coIP data are normalized with respect to signal observed for V_2R^{WT} , which is treated as 100% (Figures 4B and 5B).

Bimane fluorescence spectroscopy

We previously described a detailed protocol for bimane fluorescence spectroscopy using bimane-labeled βarr1 (Kumari et al., 2016). Essentially, purified βarr1^{L68C} was labeled with mBBr (Sigma-Aldrich), and unreacted mBBr was separated on a PD10 desalting column (GE Healthcare). For fluorescence experiments, mBBr-labeled βarr1^{L68C} was used at an approximate final concentration of 2 μM and mixed with threefold molar excess (6 μM) of purified V_2R (WT or ΔICL3) and Fab30 for 60 min at room temperature (25°C). Here V_2R was purified from agonist-stimulated cells to generate active and phosphorylated receptor. As a negative control, we also purified V_2R^{WT} from inverse agonist-treated cells (inactive and non-phosphorylated). Fluorescence scanning analysis was performed using a fluorometer (model LS-55; PerkinElmer) in photon counting mode by setting the excitation and emission band-pass filter of 5 nm. For emission scan, excitation was set at 397 nm, and emission was measured from 415 to 600 nm with a scan speed of 50 nm/min. Bimane fluorescence intensities in each experiment were normalized with respect to βarr1 plus Fab30 condition, which was treated as 100% (Figure 3, B and C). Fluorescence intensity was also corrected for background fluorescence from buffer and protein in all experiments, and each experiment was repeated at least twice.

Receptor endocytosis and ERK assay

Agonist-induced receptor internalization (Figure 4C) was measured using essentially the same protocol as described for measuring receptor surface expression. The only modification was that after serum starvation, cells were stimulated with AVP (100 nM) for indicated times. The values were normalized with respect to 0-min signal, which was treated as 100%. Data in Figure 4C represent the average \pm SEM of six independent experiments, each performed in duplicate.

For measuring agonist-induced ERK phosphorylation (Figure 5, C and D), transfected HEK-293 cells were serum starved for 4–6 h and then stimulated with 100 nM AVP for indicated times. Afterward, cells were lysed in 100 μl of 2 \times SDS loading buffer and sonicated, and lysates were separated by 12% SDS-PAGE. Subsequently Western blotting was performed to assess the phosphorylation of

ERK1/2 using phospho-ERK primary antibody (9101; Cell Signaling Technology) overnight at 4°C, followed by 1 h of incubation with anti-rabbit immunoglobulin G secondary antibody (A00098; GenScript) at room temperature. The membrane was then washed with 1× TBST three times and developed using ChemiDoc set-up (Bio-Rad). Phospho-ERK antibody was stripped off using 1× stripping buffer, and then the membrane was reprobred with total ERK antibody (9102, Cell Signaling Technology).

Data analysis

Experimental data were plotted using GraphPad Prism software. Data were analyzed using appropriate statistical analysis, as indicated in the figure legends, which also give the data normalization.

ACKNOWLEDGMENTS

We thank Ramanuj Banerjee for helping in receptor expression and Pragya Gupta for helping with the ERK assay and confocal microscopy. We thank Ashwani K. Thakur for kindly allowing us to use the fluorometer in his laboratory. Research in A.K.S.'s laboratory is supported by the Indian Institute of Technology, Kanpur; the Department of Science and Technology, Council of Scientific and Industrial Research; the Department of Biotechnology; and the Wellcome Trust/Department of Biotechnology India Alliance. A.K.S. is an Intermediate Fellow of the Wellcome Trust/Department of Biotechnology India Alliance (IA/I/14/1/501285).

REFERENCES

Bjarnadottir TK, Gloriam DE, Hellstrand SH, Kristiansson H, Fredriksson R, Schiöth HB (2006). Comprehensive repertoire and phylogenetic analysis of the G protein-coupled receptors in human and mouse. *Genomics* 88, 263–273.

Bockaert J, Pin JP (1999). Molecular tinkering of G protein-coupled receptors: an evolutionary success. *EMBO J* 18, 1723–1729.

Butcher AJ, Kong KC, Prihandoko R, Tobin AB (2012). Physiological role of G-protein coupled receptor phosphorylation. *Handb Exp Pharmacol* 79–94.

Coffa S, Breitman M, Hanson SM, Callaway K, Kook S, Dalby KN, Gurevich VV (2011). The effect of arrestin conformation on the recruitment of c-Raf1, MEK1, and ERK1/2 activation. *PLoS One* 6, e28723.

DeWire SM, Ahn S, Lefkowitz RJ, Shenoy SK (2007). Beta-arrestins and cell signaling. *Annu Rev Physiol* 69, 483–510.

Farrens DL, Altenbach C, Yang K, Hubbell WL, Khorana HG (1996). Requirement of rigid-body motion of transmembrane helices for light activation of rhodopsin. *Science* 274, 768–770.

Goodman OB Jr, Krupnick JG, Santini F, Gurevich VV, Penn RB, Gagnon AW, Keen JH, Benovic JL (1996). Beta-arrestin acts as a clathrin adaptor in endocytosis of the beta2-adrenergic receptor. *Nature* 383, 447–450.

Gurevich EV, Tesmer JJ, Mushegian A, Gurevich VV (2012). G protein-coupled receptor kinases: more than just kinases and not only for GPCRs. *Pharmacol Ther* 133, 40–69.

Gurevich VV, Gurevich EV (2004). The molecular acrobatics of arrestin activation. *Trends Pharmacol Sci* 25, 105–111.

Gurevich VV, Gurevich EV (2013). Structural determinants of arrestin functions. *Prog Mol Biol Transl Sci* 118, 57–92.

Gurevich VV, Gurevich EV (2014). Extensive shape shifting underlies functional versatility of arrestins. *Curr Opin Cell Biol* 27, 1–9.

Kang DS, Tian X, Benovic JL (2014). Role of beta-arrestins and arrestin domain-containing proteins in G protein-coupled receptor trafficking. *Curr Opin Cell Biol* 27, 63–71.

Kang Y, Gao X, Zhou XE, He Y, Melcher K, Xu HE (2016). A structural snapshot of the rhodopsin-arrestin complex. *FEBS J* 283, 816–821.

Kang Y, Zhou XE, Gao X, He Y, Liu W, Ishchenko A, Barty A, White TA, Yefanov O, Han GW, et al. (2015). Crystal structure of rhodopsin bound to arrestin by femtosecond X-ray laser. *Nature* 523, 561–567.

Kim YJ, Hofmann KP, Ernst OP, Scheerer P, Choe HW, Sommer ME (2013). Crystal structure of pre-activated arrestin p44. *Nature* 497, 142–146.

Kumari P, Srivastava A, Banerjee R, Ghosh E, Gupta P, Ranjan R, Chen X, Gupta B, Gupta C, Jaiman D, Shukla AK (2016). Functional competence

of a partially engaged GPCR-beta-arrestin complex. *Nat Commun* 7, 13416.

Laporte SA, Oakley RH, Zhang J, Holt JA, Ferguson SS, Caron MG, Barak LS (1999). The beta2-adrenergic receptor/betaarrestin complex recruits the clathrin adaptor AP-2 during endocytosis. *Proc Natl Acad Sci USA* 96, 3712–3717.

Lefkowitz RJ (2007). Seven transmembrane receptors: something old, something new. *Acta Physiol (Oxf)* 190, 9–19.

Lefkowitz RJ, Shenoy SK (2005). Transduction of receptor signals by beta-arrestins. *Science* 308, 512–517.

Lin A, DeFea KA (2013). beta-Arrestin-kinase scaffolds: turn them on or turn them off? *Wiley Interdiscip Rev Syst Biol Med* 5, 231–241.

Luttrell LM, Ferguson SS, Daaka Y, Miller WE, Maudsley S, Della Rocca GJ, Lin F, Kawakatsu H, Owada K, Luttrell DK, et al. (1999). Beta-arrestin-dependent formation of beta2 adrenergic receptor-Src protein kinase complexes. *Science* 283, 655–661.

Luttrell LM, Lefkowitz RJ (2002). The role of beta-arrestins in the termination and transduction of G-protein-coupled receptor signals. *J Cell Sci* 115, 455–465.

Luttrell LM, Roudabush FL, Choy EW, Miller WE, Field ME, Pierce KL, Lefkowitz RJ (2001). Activation and targeting of extracellular signal-regulated kinases by beta-arrestin scaffolds. *Proc Natl Acad Sci USA* 98, 2449–2454.

Manglik A, Kobilka B (2014). The role of protein dynamics in GPCR function: insights from the beta2AR and rhodopsin. *Curr Opin Cell Biol* 27, 136–143.

McDonald PH, Chow CW, Miller WE, Laporte SA, Field ME, Lin FT, Davis RJ, Lefkowitz RJ (2000). Beta-arrestin 2: a receptor-regulated MAPK scaffold for the activation of JNK3. *Science* 290, 1574–1577.

Nobles KN, Guan Z, Xiao K, Oas TG, Lefkowitz RJ (2007). The active conformation of beta-arrestin1: direct evidence for the phosphate sensor in the N-domain and conformational differences in the active states of beta-arrestins1 and -2. *J Biol Chem* 282, 21370–21381.

Puig J, Arendt A, Tomson FL, Abdulaeva G, Miller R, Hargrave PA, McDowell JH (1995). Synthetic phosphopeptide from rhodopsin sequence induces retinal arrestin binding to photoactivated unphosphorylated rhodopsin. *FEBS Lett* 362, 185–188.

Rasmussen SG, DeVree BT, Zou Y, Kruse AC, Chung KY, Kobilka TS, Thian FS, Chae PS, Pardon E, Calinski D, et al. (2011). Crystal structure of the beta2 adrenergic receptor-Gs protein complex. *Nature* 477, 549–555.

Ren XR, Reiter E, Ahn S, Kim J, Chen W, Lefkowitz RJ (2005). Different G protein-coupled receptor kinases govern G protein and beta-arrestin-mediated signaling of V2 vasopressin receptor. *Proc Natl Acad Sci USA* 102, 1448–1453.

Shenoy SK, Lefkowitz RJ (2011). Beta-arrestin-mediated receptor trafficking and signal transduction. *Trends Pharmacol Sci* 32, 521–533.

Shukla AK, Manglik A, Kruse AC, Xiao K, Reis RI, Tseng WC, Staus DP, Hilger D, Uysal S, Huang LY, et al. (2013). Structure of active beta-arrestin-1 bound to a G-protein-coupled receptor phosphopeptide. *Nature* 497, 137–141.

Shukla AK, Westfield GH, Xiao K, Reis RI, Huang LY, Tripathi-Shukla P, Qian J, Li S, Blanc A, Oleskie AN, et al. (2014). Visualization of arrestin recruitment by a G-protein-coupled receptor. *Nature* 512, 218–222.

Sinha A, Jones Brunette AM, Fay JF, Schafer CT, Farrens DL (2014). Rhodopsin TM6 can interact with two separate and distinct sites on arrestin: Evidence for structural plasticity and multiple docking modes in arrestin-rhodopsin binding. *Biochemistry* 53, 3294–3307.

Sommer ME, Farrens DL, McDowell JH, Weber LA, Smith WC (2007). Dynamics of arrestin-rhodopsin interactions: Loop movement is involved in arrestin activation and receptor binding. *J Biol Chem* 282, 25560–25568.

Sommer ME, Smith WC, Farrens DL (2005). Dynamics of arrestin-rhodopsin interactions: arrestin and retinal release are directly linked events. *J Biol Chem* 280, 6861–6871.

Srivastava A, Gupta B, Gupta C, Shukla AK (2015). Emerging functional divergence of beta-arrestin isoforms in GPCR function. *Trends Endocrinol Metab* 26, 628–642.

Szcepek M, Beyriere F, Hofmann KP, Elgeti M, Kazmin R, Rose A, Bartl FJ, von Stetten D, Heck M, Sommer ME, et al. (2014). Crystal structure of a common GPCR-binding interface for G protein and arrestin. *Nat Commun* 5, 4801.

van Koppen CJ, Jakobs KH (2004). Arrestin-independent internalization of G protein-coupled receptors. *Mol Pharmacol* 66, 365–367.

Xiao K, Shenoy SK, Nobles K, Lefkowitz RJ (2004). Activation-dependent conformational changes in beta-arrestin 2. *J Biol Chem* 279, 55744–55753.